STABILITY ANALYSIS OF AN ISOLATED MICROGRID WITH THE PRESENCE OF THE HYBRID ENERGY STORAGE SYSTEM-BASED VIRTUAL SYNCHRONOUS GENERATOR

Van Tan Nguyen[1], Thanh Bac Le[2], Quang Son Vo[1], Huu Dan Dao[1]

[1]The University of Danang, The University of Science and Technology;
tan78dhbk@dut.udn.vn, vqson@dut.udn.vn, dhdan.1997@gmail.com
[2]The University of Danang; lethanhbac@ac.udn.vn

Abstract - Nowadays, isolated microgrids formed by distributed generators based on renewable energy sources and power electronic converters have become more and more popular. There has been a lot of research for improving the stability of microgrids in recent years particularly the virtual synchronous generator (VSG) is a topic of great interest. This paper presents the stability analysis of an isolated microgrid based on wind-photovoltaic-diesel hybrid energy sources with the introduction of a proposed VSG. The proposed VSG is based on a battery-supercapacitor (SC) hybrid energy storage system aiming to maintain the stability of the studied isolated microgrid under disturbance conditions. The time-domain simulation results of the studied system under various disturbance conditions are examined to evaluate the effectiveness of the proposed VSG. It can be concluded from the simulation results that the proposed VSG can effectively compensate power fluctuations and maintain the stability of the studied microgrid under various disturbance conditions. The simulation results also show that while the battery can handle the long-term power variations, the SC can absorb the rapid power fluctuations. Thus, the proposed VSG based on a combination of the battery and the SC could improve the battery's lifetime and reduce the invested cost of the SC.

Key words - Dynamic stability; isolated microgrid; hybrid energy storage system; photovoltaic (PV) power generator; virtual synchronous generator; wind power generator

1. Introduction

The depletion of fossil fuel reserves and the issues of environmental pollution have spurred the use of more and more renewable energy, such as wind and photovoltaic (PV), throughout the world [1]. However, renewable energy sources (RESs) heavily depend on natural conditions, so their output power fluctuates stochastically. The power fluctuations injected by the RESs may result in a large imbalance between the generations and the consumption loads, which causes deviations of the frequency and voltage of the weakgrids such as isolated microgrids [2]. An emerging solution to the improvement of power quality and stability of the microgrids is the employment of a virtual synchronous generator (VSG) to emulate the behavior of a conventional synchronous generator's primary engine, thus providing the inertia and damping for a microgrid [3] - [5]. Some strategies of the advanced control and optimization of VSG parameters have been presented in [6] - [10]. However, the presented methods were only concerned with control strategies, so the VSG was implemented with constant DC voltage source and obviously not in the actual case. In fact, the energy storage system (ESS) can be equipped for the needs of the VSG to absorb and inject energy into the microgrid for suppressing power fluctuations. The studies of the VSG based on ESS which is connected to a voltage source inverter were presented in [11] - [14]. The choice of ESS technology depends on the specific applications. In this paper, a VSG based on a battery-supercapacitor (SC) hybrid energy storage system (HESS) is proposed, aiming to compensate power fluctuations, thus maintaining the stability of a wind-PV-diesel based isolated microgrid under disturbance conditions. The battery-SC HESS is a combination of a high energy density unit, i.e., the battery and a high power density unit, i.e., the SC to improve the system operating performance and increase the battery life as well as reduce the invested cost of the SC. More details about the battery-SC based HESS can be found in [15] - [17]. The effectiveness of the proposed VSG on the stability of the studied isolated microgrid under various disturbance conditions is evaluated through the time-domain simulation results. The rest of the paper is organized as follows.The configuration of the studied isolated microgrid and control scheme of the proposed VSG are presented in Section 2. The stability analysis of the VSG control loop using root-locus is depicted in Section 3. The time-domain simulation results of the studied system are analyzed in Section 4. Finally, the main conclusions of this paper are drawn in Section 5.

2. Configuration of Studied Isolated Microgrid and Control Scheme of VSG

2.1. *Configuration of the Studied Isolated Microgrid*

Figure 1 shows the configuration of the studied wind-PV-diesel based isolated microgrid. The wind power generator (WPG) is based on a permanent-magnet synchronous generator (PMSG) feeding power to the point of common coupling (PCC) through a voltage-source converter (VSC), a DC-link, and a voltage source inverter (VSI). The PV power generator (PVPG) consists of PV arrays connected to the PCC through a DC/DC boost converter, a DC-link, and a VSI. Both the WPG and the PVPG are equipped with a maximum power point tracking (MPPT) controller so that they can extract maximum power available as wind speed and solar radiance change. The details of the MPPT algorithm for the PVPG can be found in [18], [19] while the details of MPPT controller of the WPG can be referred to in [20] - [22]. The diesel generator, as shown in Figure 1, is directly connected to the PCC. In this paper, the load is modelled as a constant power load. To improve the stability of the studied isolated microgrid, a VSG based on a battery-SC HESS is proposed. The battery and the SC are coupled at a common DC-link using bidirectional DC/DC converters. A VSI which is equipped with a VSG controller is used to interface the common DC-

link with the microgrid. The VSG is controlled to support the inertia power for improving the frequency responses of the microgrid. The details of the VSG's control scheme are presented hereafter in next subsection.

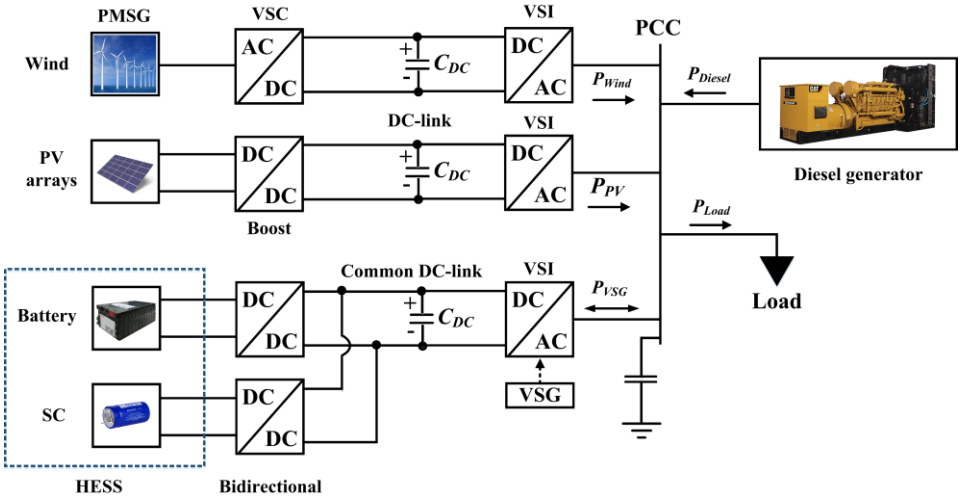

***Figure 1**. Configuration of the studied isolated microgrid*

2.2. *Control Scheme of the VSG*

Figure 2 illustrates the control scheme of the VSG which consists of the controller for the VSI and the common DC-link voltage controller.

The control of the VSI aims to enable the VSG to absorb power fluctuations for enhancing the frequency responses of the microgrid and to maintain the voltage of the PCC. The controller for the VSI shown in Figure 2 comprises the VSI control block and the proposed VSG control block. In fact, this controller is the modification of the conventional controller of the VSI by adding the proposed VSG control loop aiming to provide virtual inertia and damping for the studied isolated microgrid. The detailed model of the conventional controller of the VSI can be referred to [23], while the additional VSG control loop is discussed hereafter.

Figure 3 shows the control block diagram of the proposed VSG control loop. In this figure, the swing equation that mimics the behavior of a synchronous generator is expressed in per-unit as follows:

$$T_m - T_{out} = 2H\frac{d\omega_{VSG}}{dt} + D(\omega_{VSG} - \omega_{ref}) \quad (1)$$

where $T_m$is the mechanical torque of the VSG; T_{out} is the output electromagnetic torque of the VSG; ω_{VSG} and ω_{ref} are the angular frequency of the VSG and the reference angular frequency, respectively; H and D are the inertia constant and damping factor of the VSG, respectively.

In order to share steady-state active power, a droop control is added to the VSG control loop for calculating the mechanical torque of the VSG, the per-unit mechanical torque of the VSG is given by

$$T_m = (P_{m0} + \Delta P_m)\frac{1}{\omega_{ref}} = [P_{m0} + \frac{1}{R_d}(\omega_{ref} - \omega_e)]\frac{1}{\omega_{ref}} \quad (2)$$

where P_{m0} is the initial mechanical power of the VSG; ω_e is the angular frequency of the microgrid; R_d is the droop constant.

In Figure 3, a secondary control loop with gain k_{id} is also considered aiming to recover the frequency of the microgrid to its nominal value under dynamic conditions.

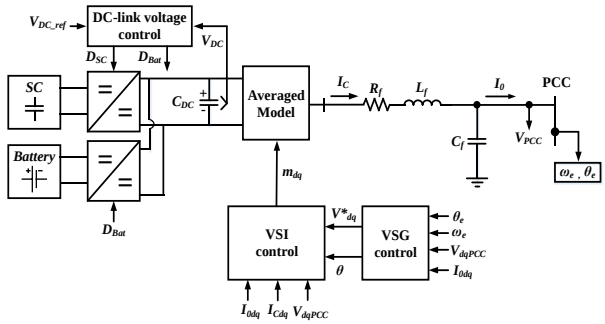

***Figure 2.** Control scheme of the VSG*

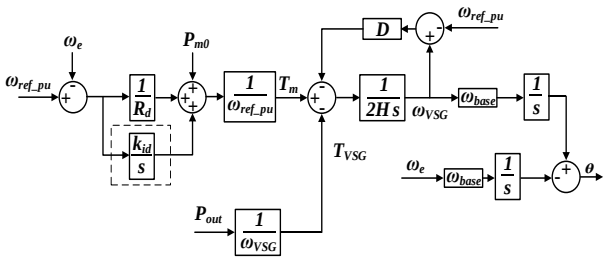

***Figure 3.** Control block diagram of the VSG control loop*

To maintain the voltage of the PCC bus, the VSG is also equipped with a voltage control loop which generates the reference voltage for the inner VSI control loop. The mathematical equation of the voltage control loop can be written by

$$K\frac{dV^*}{dt} = (V_{PCC\_ref} - V^*)D_q + Q_0 - Q_{out} \quad (3)$$

where Q_0 and Q_{out} are the reference reactive power and the output reactive power of the VSI, respectively; D_q is the voltage droop coefficient; V^* is the reference voltage value generated by the voltage control loop, $V_{PCC}$is the voltage of the PCC; K is the voltage integral coefficient.

Figure 4 depicts the control block diagram of the common DC-link voltage controller of the VSG aiming to maintain the constant DC-link voltage (V_{DC}) [14]. To maintain the common DC-link voltage constant, the HESS must be controlled to absorb power imbalance at the common DC-link which is caused by the demand from the VSI. The PI controller which is employed to regulate the common DC-link voltage error generates the total reference current(I_{HESS_ref}) required for the HESS. Because of the fast dynamic response characteristic of the SC and the long-term energy storage capability of the battery, a low-pass filter with the time constant T_s is used to filter out the slowly varied current that is used as the reference current I_{bat_ref}forthe inner current-control loop of the battery. The remain high-frequency signal is used as the reference signal$I_{sc_ref}$for the inner current-control loop of the SC. The inner current-loops process the current errors and generate the required duty cycles for each bidirectional DC/DC converter.

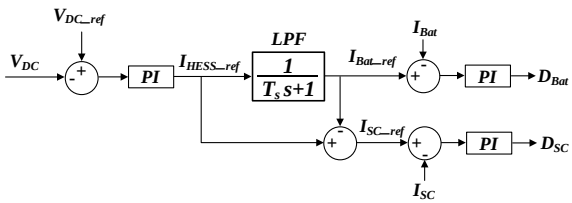

Figure 4. *Control block diagram of DC-link voltage controller*

3. Stability Analysis of the VSG Control Loop

In this section, the small-signal stability analysis of the VSG control loop is presented. According to [24] and referring to Figure 2, the output active power of the VSG can be expressed by

$$P = \frac{(EV_{PCC}\cos\theta - V^2_{PCC}R_f + EV_{PCC}X_f\sin\theta)}{(R^2_f + X^2_f)} \quad (4)$$

The above active power equation is analyzed by applying small-signal disturbancesat the operating point of the power angle θ, it is conducted as follows:

$$\Delta P = \frac{\partial P}{\partial\theta}\Delta\theta = \frac{EV_{PCC}X_f\cos\theta - EV_{PCC}R_f\sin\theta}{R^2_f + X^2_f}\Delta\theta$$

$$= K\Delta\theta \quad (5)$$

The transfer function of the frequency-active power control of the VSG is illustrated in Figure 5. The root-loci obtained from the small-signal model of the VSG control loop are plotted Figure 6.

Figure 6(a) demonstrates the root-locus plot of the VSG control loop when inertia constant H = 4 sand the damping factor D increases from 0 to 200. It is seen that when the damping factor is equal to zero, the two poles of the transfer function are located on the imaginary axis, which means the system is at the stable boundary. When the damping factor increases, the two poles move to the left-hand side of complex plane indicating that the system becomes more stable. Figure 6(b) shows the root-locus plot of the VSG control loop when the damping factor D = 20 and the inertia constant H change from 0 to 10 s. It is clearly observed that when the inertia constant increases the poles of the system move towards the imaginary axis, which means that the stability of the system is degraded at higher value of the inertia constant. However, the system is still stable for all examined values of the inertia constant since the root loci shown in Figure 6(b) are entirely located on the left-hand side of the complex plane.

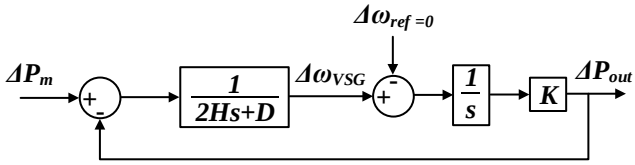

Figure 5. *Small-signal model of the VSG control loop*

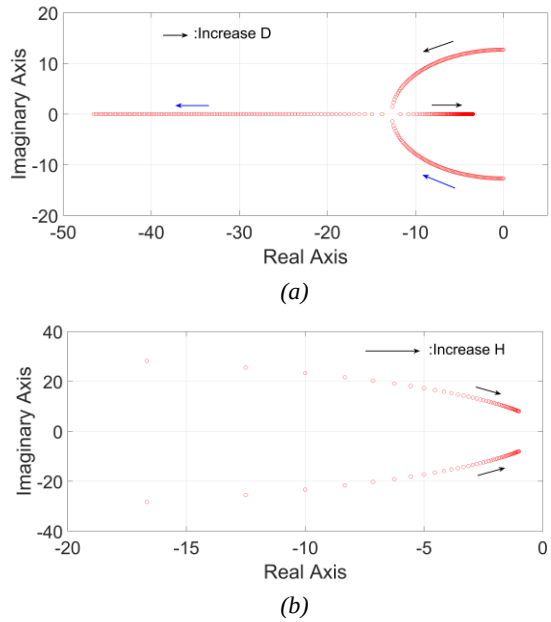

Figure 6. *Root-loci of the VSG control loop*

4. Time-Domain Simulation Results

In this section, the stability of the studied isolated microgrid with the inclusion of the proposed battery-SC hybrid energy storage system based VSG under disturbance conditions is investigated using time-domain simulation results. The simulations results of the studied microgrid are carried out using Matlab/Simulink software. The main parameters of the studied system are listed in Table I. Some parameters are expressed in per-unit (pu). The base power is chosen equal to the maximum active power of load, i.e., S_{base} = 1.2 MVA.

The studied isolated microgrid is simulated under the scenario in which both variations of solar radiance and

wind speed are simultaneously applied to the PVPG and the WPG, respectively. Also, there is an event of an additional load connection causing the load demand to increase from 0.8 pu to 1.0 pu at t = 300 s (1.0 pu corresponding to 1.2 MW).

Table 1. Main parameters of the studied system.

Microgrid
P_{PV_nom} = 300 kW, P_{wind_nom} = 200 kW, P_{diesel_nom} = 1.8 MW, P_{load_max} = 1.2 MW, C_{SC} = 10 F, C_{Bat} = 600 Ah
DC-link and VSI of VSG system
V_{DC} = 1000 V, C_{DC} = 0.2 F, R_f = 1.63 mΩ, L_f = 100 µH, C_f = 2500 µF
VSG
R_d = 0.05, H = 3 s, D = 20 pu; k_{id} = 10, ω_{base} = 314.16 rad/s, ω_{ref}= 1.0 pu, V_{PCC_ref} = 1.0 pu; D_q = 166.7, K = 12

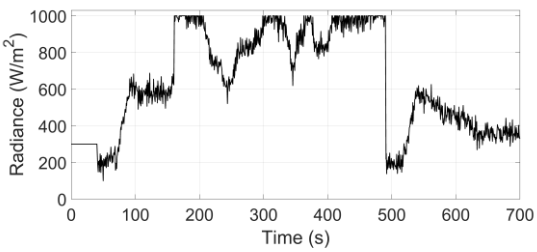

(a)

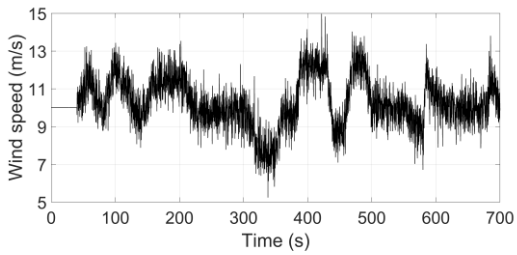

(b)

Figure 7. *Variations of solar radiance and wind speed*

Figure 7(a) and 7(b) depict the variations of applied solar radiance and wind speed, respectively. It should be noticed from Figure 7(a) that there is a sharp increase of solar radiance from 600 W/m^2 to 1000 W/m^2 at t = 160 s and a sudden decrease of solar radiance from 1000 W/m^2 to 200 W/m^2 at t = 490 s. The wind speed variations shown in Figure 7b consist of both gradual variations between 7 m/s and 13 m/s and high-frequency noise variations.

Figure 8(a) and Figure 8(b) illustrate the output powers of the PVPG and the WPG, correspondingly. It is clearly seen from Figure 8(a) and 8(b) that the output powers of the PVPG and the WPG are varied corresponding to the variations of the solar radiance and the wind speed that are shown in Figure 7(a) and 7(b).

Figure 9 demonstrates the frequency responses of the studied isolated microgrid. Due to the applied disturbances, the frequency of the studied microgrid is continuously fluctuated. It is noticed that there are sudden deviations of the frequency from the nominal frequency at times t = 160 s, 300 s, and 490 s, corresponding to the events of sharp increase of the solar radiance, the load-connection, and the sudden decrease of the solar radiance, respectively. However, it is seen that the frequency responses of the microgrid can be quickly recovered and always be maintained around the nominal frequency of 50 Hz. In other words, the studied isolated microgrid is stable under the various disturbance conditions.

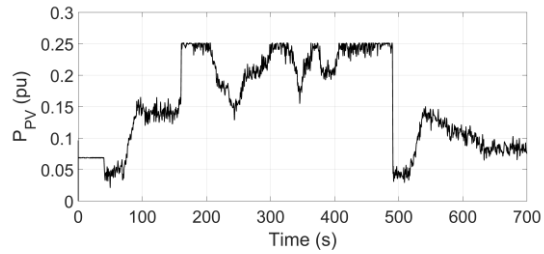

(a)

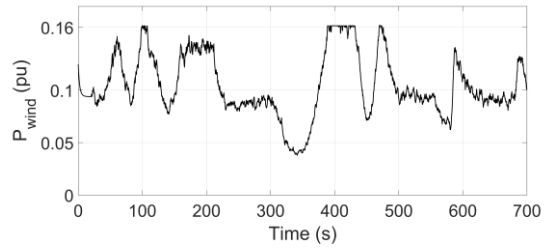

(b)

Figure 8. *Output powers of thePVPG and the WPG*

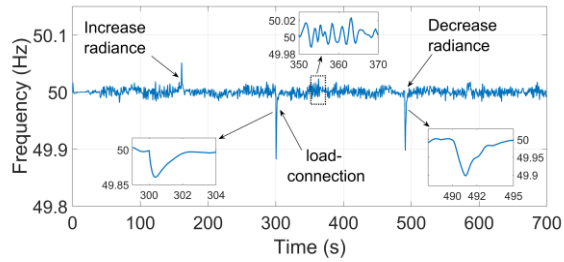

Figure 9. *Frequency responses of the microgrid*

Figure 10 and Figure 11 illustrate the power responses of the diesel generator and the proposed VSG, respectively. It is seen that both the diesel generator and the proposed VSG are responding to the power fluctuations caused by the applied disturbances. However, it can be clearly observed from Figure 10 and Figure 11 that the power responses of the diesel generator are much slower than those of the proposed VSG. On the other hand, the proposed VSG can rapidly compensate the power fluctuations, thus, ensuring the power balance between the load demand and the generated power. Moreover, the implementation of the proposed VSG in the studied microgrid can also reduce the stress on the diesel generator under disturbance conditions since rapid power fluctuations can be handled by the proposed VSG. Therefore, it can be concluded that the proposed VSG, which emulates the inertia and damping characteristic of a conventional synchronous generator, can effectively maintain the stability of the studied isolated microgrid under disturbance conditions.

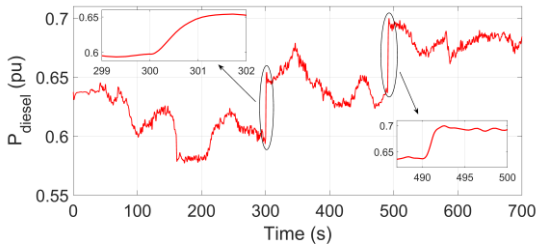

Figure 10. *Power responses of the diesel generator*

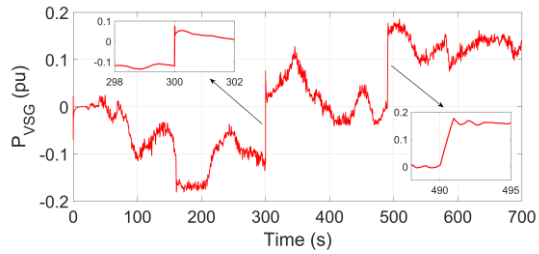

Figure 11. *Power responses of the VSG*

The dynamic response of the common DC-link voltage of the VSG is shown in Figure 12. It is seen that the voltage of the common DC-link of the VSG can be maintained almost constant at its nominal value of 1000 V under all examined disturbances.

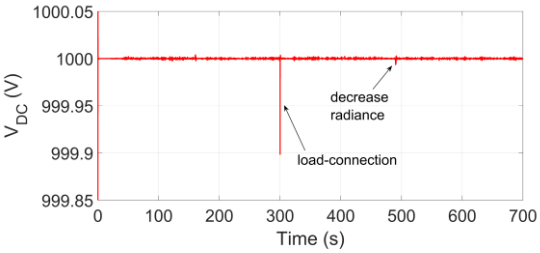

Figure 12. *Voltage of the common DC-link of the VSG*

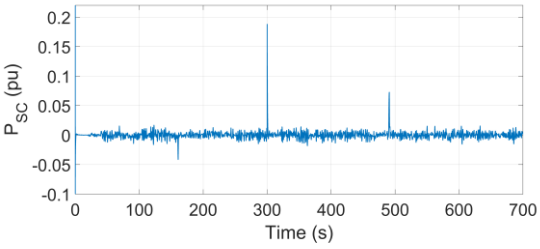

Figure 13. *Power of the SC*

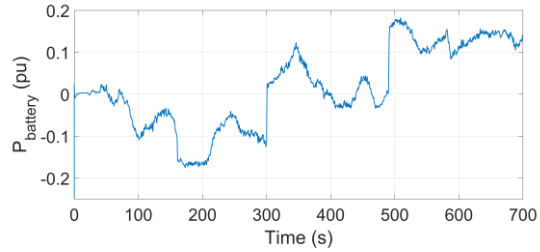

Figure 14. *Power of the battery*

Figure 13 and Figure 14 illustrate the power responses of the SC and the battery, respectively. It can be clearly observed from Figure 13 and Figure 14 that the SC can effectively compensate for the rapid and large-magnitude power fluctuations while the battery only responds for the long-term power variations. Therefore, the combination of the SC and the battery for being implemented as a VSG would prolong the battery's lifetime and reduce the invested cost of the SC.

5. Conclusions

This paper has presented the stability analysis of an isolated microgrid based on wind-PV-diesel hybrid energy sources. A virtual synchronous generator based on a battery-SC hybrid energy storage system has been proposed aiming to maintain the stability of the studied isolated microgrid under disturbance conditions. The time-domain simulation results of the studied system have been carried out to examine the effectiveness of the proposed VSG. It can be concluded from the simulation results that the proposed VSG based on a battery-SC hybrid energy storage system can effectively maintain the stability of the studied isolated microgrid under various disturbance conditions. Moreover, it can also be concluded from the simulation results that the combination of SC and battery for being implemented as a VSG in a wind-PV-diesel isolated microgrid could give excellent performance. While the SC can handle rapid power fluctuations, the battery is only responsible for long-term power variations which could significantly enhance the battery's life and reduce the cost of the SC.

Acknowledgment: This research is funded by Funds for Science and Technology Development of The University of Danang under project number B2019-DN02-73.

REFERENCES

[1] A. Anzalchi and A. Sarwat, "Analysis of carbon tax as an incentivetoward building sustainable grid with renewable energy utilization", in *Proc. 2015 7th Annual IEEE Green Technologies Conferrence (GreenTech)*, pp. 103–109.

[2] V. T. Nguyen, D. H. Hoang, H. H. Nguyen, K. H. Le, T. K. Truong, and Q. C. Le, "Analysis of uncertainties for the operation and stability of an islanded microgrid", in *Proc.2019 International Conference on System Science and Engineering (ICSSE)*, 20-21 July 2019.

[3] J. Driesen and K. Visscher, "Virtual synchronous generators", in *Proc. IEEE Power Energy Soc. Gen. Meeting—Convers. Del. Elect. Energy 21st Century*, pp. 1–3,Jul. 2008.

[4] H.P. Beck and R. Hesse, "Virtual synchronous machine", in *Proc. 9th Int. Conf. Elect. Power Qual. Util. (EPQU)*, pp. 1–6, 9-11 Oct. 2007.

[5] U. Tamrakar, D. Shrestha, M. Maharjan, B. Bhattarai, T. Hansen, & R. Tonkoski, "Virtual inertia: current trends and future directions", *Applied Sciences (Switzerland)*, vol. 7, no. 7, 2017, pp. 1-29.

[6] N. Soni, S. Doolla, and M. C. Chandorkar, "Improvement of transient response in microgrids using virtual inertia", *IEEE Trans. Power Delivery*, vol. 28, no. 3, pp. 1830-1838, July 2013.

[7] A. B. Chowdhury, X. Liang, and H. Zhang, "Fuzzy-secondary-controller-based virtual synchronous generator control scheme for interfacing inverters of renewable distributed generation in microgrids", *IEEE Trans. Industry Applications*, vol. 54, no. 2, pp. 1047-1061, March-April 2018.

[8] B. Rathore, S. Chakrabarti, and S. Anand, "Frequency response improvement in microgrid using optimized VSG control", in *Proc.2016 National Power Systems Confererence (NPSC)*, 19-21 Dec. 2016.

[9] J. A. Suul, S. D'Arco, and G. Guidi, "Virtual synchronous machine-

based control of a single-phase bi-directional battery charger for providing vehicle-to-grid services", *IEEE Trans. Ind. Appl*., vol. 52, no. 4, pp. 3234–3244, Jul./Aug. 2016.

[10] X. Hou, Y. Sun, X. Zhang, J. Lu, P. Wang, and J. M. Guerrero, "Improvement of frequency regulation in VSG-based acmicrogrid via adaptive virtual inertia", *IEEE Trans. Power Electronics*, vol. 35, no. 2, pp. 1589-1602, Feb. 2020.

[11] J. Fang, Y. Tang, H. Li, and X. Li, "A battery/ultracapacitor hybrid energy storage system for implementing the power management of virtual synchronous generators", *IEEE Trans. Power Electronics*, vol. 33, no. 4, pp. 2820-2824, April 2018.

[12] H. S. Hlaing, J. Liu, Y. Miura, H. Bevrani, and T. Ise, "Enhanced performance of a stand-alone gas-engine generator using virtual synchronous generator and energy storage system", *IEEE Access*, vol. 7, pp. 176960-176970, Dec. 2019.

[13] D. Leng, S. Polmai, "Virtual synchronous generator based on hybrid energy storage system for PV power fluctuation mitigation", *Appl. Sci. 2019*, vol. 9, no. 23, pp. 1-18, Nov. 2019.

[14] A. Anzalchi, M. M. Pour, and A. Sarwat, "A combinatorial approach for addressing intermittency and providing inertial response in a grid-connected photovoltaic system", *Power& Energy Society, IEEE General Meeting*, pp. 1-5, 17-21 Jul. 2016.

[15] V. M. M.-Marcos, M. A. G.-Martínez, F. B.-González, and M. I. M.-Montero, "A grid connected photovoltaic inverter with battery-supercapacitor hybrid energy storage", *Sensor Article*, vol. 17, no. 8, pp. 1-8, Aug. 2017.

[16] S. K. Kollimalla, M. K. Mishra, A. Ukil, and H. B. Gooi, "DC grid voltage regulation using new HESS control strategy", *IEEE Trans. Sustainable Energy*, vol. 8, no. 2, pp. 772-781, April 2017.

[17] M. Bahloul and S. K. Khadem, "Impact of power sharing method on battery life extension in HESS for grid ancillary services", *IEEE Trans. Energy Conversion*, vol. 34, no. 3, pp. 1317-1327, Sept. 2019.

[18] B. N. Nguyen, V. T. Nguyen, M. Q. Duong, K. H. Le, H. H. Nguyen, and A. T. Doan, "Propose a MPPT algorithm based on thevenin equivalent circuit for improving photovoltaic system operation. front", *Energy Res*, vol. 8, pp. 1-14, Feb. 2020.

[19] B. N. Nguyen, V. T. Nguyen, T. B. T. Truong, V. K. Pham, D. H. Hoang, and H. V. P. Nguyen, "A new maximum power point tracking algorithm for the photovoltaic power system", in *Proc. 2019 International Conference on System Science and Engineering (ICSSE)*, 20-21 Jul. 2019.

[20] M. E. Haque, M. Negnevitsky, and K. M. Muttaqi, "A novel control strategy for a variable-speed wind turbine with a permanent-magnet synchronous generator", *IEEE Trans. Industrial Applications*, vol. 46, no. 1, pp. 331-339, Jan./Feb. 2010.

[21] M. A. Abdullah, A. H. M. Yatim, and C. W. Tan, "A study of maximum power point tracking algorithms for wind energy system", in *Proc. 2011 IEEE First Conf. Clean Energy and Technology*, pp. 321-326.

[22] L. Wang, Q. S. Vo, A. V. Prokhorov, "Stability improvement of a multimachine power system connected with a large-scale hybrid wind-photovoltaic farm using a supercapacitor", *IEEE Trans. Industry Applications*, vol. 54, no. 1, pp. 50-60, Jan.-Feb. 2018.

[23] J. Liu, Y. Miure, H. Bevrani, T. Ise, "Enhanced virtual synchronous generator control for parallel inverters in microgrids", *IEEE Trans on Smart Grid*, vol. 8, no. 5, pp. 2268-2277, Sep. 2017.

[24] G. Yao, Z. Lu, Y. Wang, M. Benbouzid, and L. Moreau, "A virtual synchronous generator based hierarchical control scheme of distributed generation systems", *Energies 2017*, vol. 10, no. 12, pp. 1-23, Dec. 2017.

(The Board of Editors received the paper on 15/4/2020, its review was completed on 15/6/2020)